

Investigating Tool Wear, Chip Behaviour and Spring Back Action Using FEM

Tarek El-Hossainy¹, Mahmoud Abdrabou², Abdallah Abdelkawy³

^{1,2}Professor, Mechanical Design and Production Department, Faculty of Engineering, Cairo University

¹Professor, Industrial Systems Engineering Department, Faculty of Engineering, MSA University

³Assistant Professor, Mechanical Design and Production Department, Faculty of Engineering, Cairo University

E-mail: ¹telhossainy@hotmail.com, ²mahmoud.abdrabou@gmail.com,
³abdallah.abdelkawy@ejust.edu.eg

Abstract

The tool wear found in machining processes represents main obstacle for machinability due to its detrimental effects on surface roughness, material removal rate and machining economy. A nonlinear thermomechanical finite element model was developed to simulate the tool chip interaction. This model predicts not only the chip morphology and chip flow direction, cutting forces values, stress distribution, but also can use to predict tool wear. Furthermore, the effect of elastic deformation (spring back) and the thermal effect have been considered in the model. Cutting force was predicted and compared with the conducted experimental work. Dry turning operation was carried out on low carbon steel using carbide tool. The tool/workpiece interface stress on flank face was calculated and compared with the FEM. Predicted results show good correlation with the FEM. FE model was verified experimentally by measuring the cutting force. The friction on the flank face and spring back concentrates the stress on the flank face.

Keywords: Sliding wear, cutting force, cutting tools, spring back



1. Introduction

Machining processes are essential shaping processes for obtaining designed geometries and surface properties by shearing the workpiece material into a chip. This chip is carried out through large strain, high strain rate and hence high temperature due to adiabatic heating [1]. The generation the cutting temperature softens the cutting tool which increases the tool wear and reduces the tool life. Coating the cutting tools reduces the cutting temperature due to the reduction of the tool-workpiece friction this variation in the cutting friction required FE tool to simulate it accurately [2].

Haddag and Nouari [3] studied tool wear and heat transfer analyses in dry machining based on multi-steps numerical modelling. They obtained cutting forces, chip morphology and chip flow direction as well as tool–chip interface parameters in the first step and the second step concerns the tool wear prediction using tool–chip interface parameters. They found that the predicted tool wear highly localized at the cutting edge, particularly at the tool corner. A. Malakizadi et al. [4] carried some steps composed from experimental work, response surface methodology and FE to determine the Jonson-Cook material parameters for 1080 plain carbon steel, AA6082-T6 aluminium alloy and Inconel 718. They used DEFORM FE code to carry 2D model to determine the cutting forces and hence the coefficient of friction. C. Montenegro et al. [5] investigated the effect of low and high strain rate on the material microstructure. They used a plane strain machining which is similar to shaping process for investigated the effect of high strain rate. They got good agreement between the grain size expected from FE and the experimental results.

Zhu et al. [6] studied tool wear characteristics in machining and concluded that tool wear is generally considered to be a result of mechanical (thermo-dynamic wear, mostly abrasion) and chemical (thermo– chemical wear, diffusion) interactions between the tool and workpiece. Furthermore, it can be summarized that in metal cutting, the actual wear rate is the combination of adhesion, abrasion, diffusion, and oxidation wear rate, depending on the temperature and stress distributions. Sayit et al. [7] showed that abrasive, adhesion and oxidation wear mechanisms are predominant in the machining of continuous and interrupted cutting of ductile iron. El-Gallab and Sklad [8] Included that the interaction of the thermal and mechanical tool/chip in the model and found that the crater wear, pitting, and chipping can be predicted by their model. M. Binder et al. [9] developed the first FE model for the tool wear in metal cutting for coated complex micro tools. They proposed technique by which the cutting zone on a real cutting tool was used to make the modelled tool to be more similar to the real one. The wear of both flank and rake faces were calculated.

Mao et al. [10] presented a finite element model for simulating the temperature field in the wet surface grinding. The model takes into account the

nonlinear nature of the workpiece material properties with temperature. Their simulation demonstrates that more convincing results are obtained using the parabolic than the triangular heat-flux distribution. Wang et al. [11] developed a finite element model to simulate the cutting process and reflects the effects of high temperature, large strain, and strain rate to the workpiece material. They deduced the relationship between cutting force coefficients and chip thickness. To validate the accuracy of the model, force is predicted and shown to match the real measured force with satisfactory accuracy. Q. Xia et al. [12] modelled the cutting temperature for high speed machining using FE method. They developed their model based on quasi-static conditions due to their assumption that a thermal equilibrium occurs near the cutting tip in few seconds.

Li [13] found that tool wear in cutting process is produced by the contact and relative sliding between the cutting tool and the workpiece, and between the cutting tool and the chip under the extreme conditions of cutting area. Yen et al. [14] estimated tool wear in orthogonal cutting using the finite element analysis. They discussed the numerical implementation of the integration of tool wear models with FEM calculations to predict the evolution of wear over long cutting periods. Both researchers [13], [14] found that the simulations using a cutting tool with constantly updated rake face and flank face geometries have shown that it is possible to predict the evolution of tool wear at any given cutting time from FEM simulations by using the methodology proposed in their study.

Attanasio et al. [15] mentioned that previous performed researches showed some problems in the correct identification of crater depth and position when using analytical tool wear models based only on abrasive or diffusive tool wear mechanisms. They added that they implemented a new analytical tool wear model, taking into account the influence of both abrasive and diffusive tool wear mechanisms for overcoming these limits. D. Yang et al. [16] suggested a sequence composed of FE (Abaqus/Explicit simulation) and statistical analysis to optimize the residual stress during milling process. They simplified the milling process similar to shaping process with variable undeformed chip thickness as Sin function of the undeformed chip thickness and the end mill rotation angle. They verified both FE and regression model using experimental machining on α and β phase titanium alloy TI05Al-4V.

Thepsonthi and Ozel [17] employed FE simulations to investigate chip formation process in terms of cutting force generation, tool temperature and contact pressure, sliding velocity and hence tool wear rate. They mentioned that the simulation results were further utilized for estimating tool life using a sliding wear rate model. Vadiraj et al. [18] studied the Effect of sliding speed on wear behaviour. They found that under dry condition, wear loss increases and friction coefficient decreases with sliding speeds.



Grzesik and Nieslony [19] studied the tool-chip contact behaviour using FEM-based modelling. They found that their simulation approach can be seen in elaborating more accurate models with updated thermal properties. Particularly, it contributes to predicting some fundamental relationships between all physical phenomena involved into the overall tool-chip contact behaviour.

Lorentzon and Jarvstrat [20] concluded that the proposed friction description with a lower coefficient in the area around the tool tip together with Usui's [21] empirical wear equation shows excellent experimental agreement where coulomb friction model commonly employed.

Arcona and Dow [22] mentioned that During the metal cutting processes, the cutting force applied on the cutting tool is related to the elastic deflection, or spring back of the workpiece. Moreover, thrust force is deduced due to the frictional forces on the tool rake face and the normal force associated with spring back.

Fang et al. [23] stated that after the work material has passed the lowest cutting edge point, the elastic portion springs back and that the elastic portion springs back. Workpiece hardness, shear angle or chip-tool friction coefficient, elastic deformation force of the workpiece are needed for calculating the total tool force [16]. Ozturk et al. [24] measured the elastic energy of the material at various temperatures under tensile loading condition. Their results reveal that the spring back is substantially reduced with increasing temperature. Jiang and Chen [25] studied the spring back behaviour of the Microtube and found that the experimental springback result was higher than that of the prediction made by the simulation for the occurrence of grain subdivision, induced by strain hardening, reduced the spring back amount.

The cutting tool conditions are significant factors in machining process so, many researchers directed to build FE models to study these conditions. F. Ducobu et al. [26] built a 3D finite element (FE) model to close the FE model to the real experiments. They verified their model by machining a Ti6Al4V alloy using WC/Co tool coated with TiV PVD. The tool was modelled by the Lagrangian formalism and the workpiece was modelled by Eulerian. Their model expressed the cutting force accurately. S. Kumar et al. [27] investigated the effect of textured cutting tool on the cutting force and chip-tool contact length using 3D FE using AdvantEdge 3D software which used lagrangian dynamic explicit. They investigated different shapes of textures as circular, rectangular, triangular and elliptical. The model was built to simulate turning of Ti6Al4V titanium alloy. They found that the textured area affected significantly on the cutting force while the shape of texture effect came the second.

The objective of this study is to predict the chip morphology and chip flow direction, cutting force values, stress distribution, and predict tool wear evolution taking into consideration the spring back action using FEM simulations.

2. Finite Element Model

A finite element model was developed for simulating the cut and uncut chip thicknesses during machining processes. This was carried out using ABAQUS/CAE software using the elements of isoparametric quadrilateral. Sliding friction between the deformed chip and cutting tool face have been studied. The process simulation was carried out as movement of the cutting tool against the workpiece which is prevented to move from the left and bottom sides like the shaping process. These steps allow obtaining stable cutting forces and accurate chip morphology [3]. The slideline was used to perform the separation of rake face and uncut chip nodes. This slidelines movement is constrained to prevent the nodes form interfering and give chance to simulate the friction between the contact surfaces.

Carbide cutting tool material with a 27.5° rake angle was used during the machining process and the undeformed chip thickness was 0.25 mm. The cutting speed was 200 m/min and the workpiece materials conditions were 0.2% carbon, with modulus of elasticity $E = 2.1 \times 10^5$ N/mm², and 0.3 Poisson ratio. The calculated values of the effective stress and strain hardening coefficient so that the effective stress of 836 N/mm² and the strain hardening coefficient of 0.036 were applied in the FE model [28]–[30].

3. Spring back Action

The investigation of material spring back demonstrated an empirical model to describe this phenomenon. These parasitic forces were attributed to elastic spring back of the workpiece as it is compressed and moved under the cutting edge without being removed [31]. The spring back can be represented shown in equation (1) [31], [32]:

$$S = K1r \frac{H}{E} \quad (1)$$

Where S is the deflection of the machined surface or spring back, K1 is a scaling constant for the best fit for Eq. (1), r is the cutting tool nose radius, H is the workpiece hardness and E is the modulus of elasticity where $H/E = 0.04$ [33]. Spring back action was calculated from Eq.(1) and applied in the FE model.

The thrust force which is deduced form the cutting tool sliding over the workpiece was used to calculated the contact stress of the elastic spring back by



dividing the thrust force values by the estimated area due to spring back [22]. The contact stress can be expressed as a function of hardness divided by elastic modulus. An experimental relationship for this tool/workpiece interface stress on flank face [31], [32] is given by:

$$\sigma = K_2 H \sqrt{\frac{H}{E}} \quad (2)$$

Where k_2 is a scaling constant. The measured shear angle was used to compute a coefficient of rake friction at the tool/chip interface is from the following equation [22].

$$\mu = \frac{\cos \phi - \frac{\sin \phi}{\sqrt{3}}}{\frac{\cos \phi}{\sqrt{3}} + \sin \phi} \quad (3)$$

4. Experimental Work

Some experiments were carried out using a centre lathe for machining low carbon steel using carbide cutting tool in without coolant machining. The cutting speed was 200 m/min and the uncut chip thickness was 0.25 mm. A homemade dynamometer for two component force was used for measuring cutting forces. The dynamometer specifications were: maximum force was 3000 N, with a sensitivity of ± 1 N and natural frequency of 2 kHz. The dynamometer was calibrated using a proving ring which is characterized with maximum load of 2920 N with an elastic constant of 1460 N/mm.

5. Results and Discussion

In this model, the chip formation process was simulated with steps performed by Abaqus program. The effect of elastic deformation of the workpiece (spring back) has been considered and the thermal effect was included in the model.

Figure 1 demonstrates the start of separation of chip from workpiece and tool showing the formation of chip. It reveals that the chip is leaving the tool rake face due to chip curl as a result of the friction between chip and tool. It also shows an early predicted flank wear as proved by the stress concentration at the flank face of the tool. The stress concentration at the flank face occurred as a result of the friction between the tool flank face and the machined surface added to the spring back effect as was included in the model. Flank wear zone is predicted and the tool wear is highly localized at the nose of the cutting edge as verified by the tool wear experimental result shown in Figure 2. Finally, the predicted tool wear is highly localized at the cutting edge as found by Haddag and Nouari [3].

In Figure 3, the start of predicted crater wear is very clear as an indication of the flow of chip directed towards the tool face with the friction force acting between the chip and tool face. The crater wear is well identified on the tool face by the stress concentration at about 0.2 mm from the tool tip due to abrasive and diffusive wear mechanisms. Also, the deformation at the free end of shear plane gives an indication of micro-fissure formation at the chip at that end.

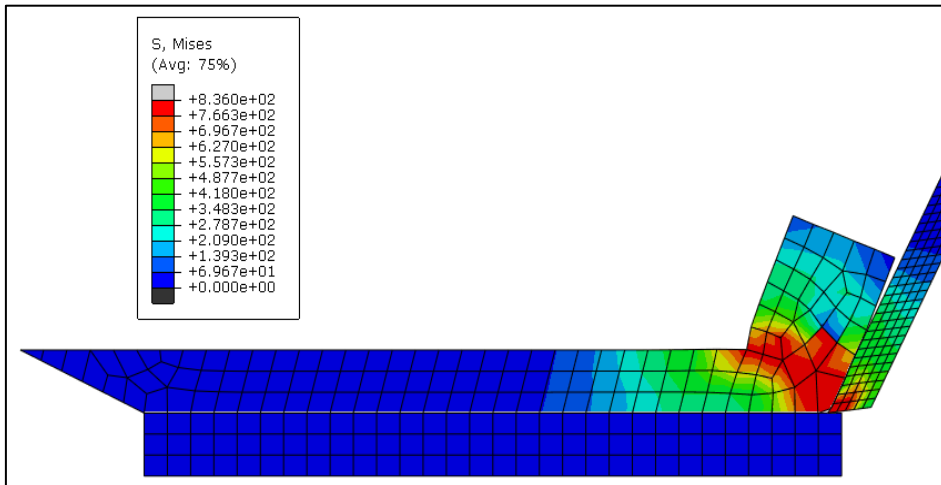


Figure 1. Developed Von-Mises stress by the start of chip removal (Travel = 0.059 mm.)



Figure 2. Carbide cutting edge with flank wear.

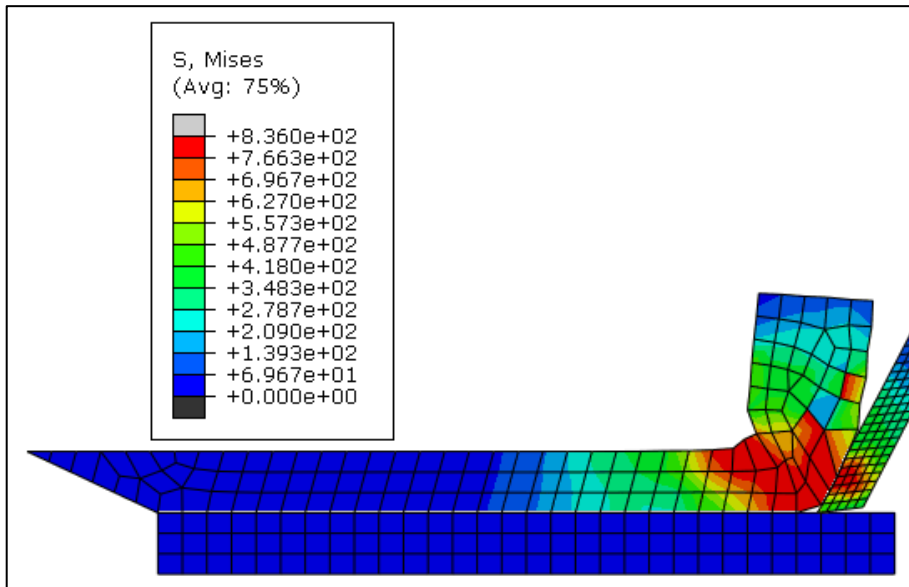


Figure 3. The start of predicted crater wear (Travel = 0.315 mm.)

In Figures 4-5, as cutting proceeds, fissures at the free end of shear plane are continuously possibly occurs. Chip curl is clearly initiated due to the presence of friction between chip and tool face. As cutting proceeds, flank wear and crater wear is actually a cumulative process increasing till tool blunt. It is clear also, the stress affected zone in the workpiece before shear plane which seems to be constant as cutting proceeds.

Figures 6-8 shows that as cutting proceeds, stresses on tool face are variable with the chip curl. The chip curl could be clearly extracted from the behaviour of chip along cutting. These figures do not show constant crater and flank wear. This may be due to the effect of chip curl which in turn the stress concentration varied with the increase of curvature in chip formation. The crater wear and flank wear could be clearly predicted from the results of the stress distribution along the tool rake face and the flank face respectively.

Finally, as cutting proceeds, chip curl increases, shear angle decreases, variation of tool wear as it is commutative, fissures at the shear plane free end, and stresses distribution on tool face are variable with the chip curl.

To verify the model, the experimental results show cutting force of 523 N while the FEM results in cutting force of 494 N at the same conditions of the experiments. The difference in cutting force value could be due to the effect of tool

wear. Also, the tool/workpiece interface on flank face stress σ calculated by Eq. 2 is 820 MPa while the FEM gives σ reached between 766 and 836 MPa.

Figure 9 shows the energy relation between the external work, internal energy (plastic dissipation) and the frictional dissipation. It reveals that the exerted external work input to the model equals to the internal energy which is the plastic dissipation in addition to the frictional dissipation in the rake and flank faces. Figure 10 gives the relation between the frictional dissipation and the travel of tool. This relation is very important in predicting the tool wear.

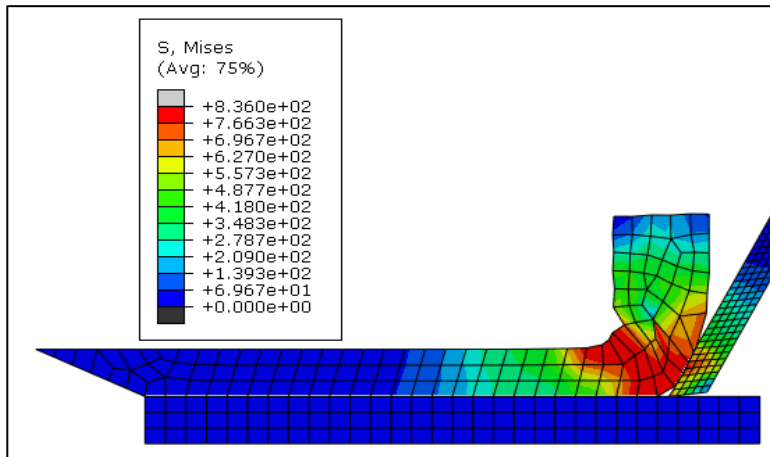


Figure 4. Predicted stresses at the free end of shear plane (Travel = 0.44 mm.)

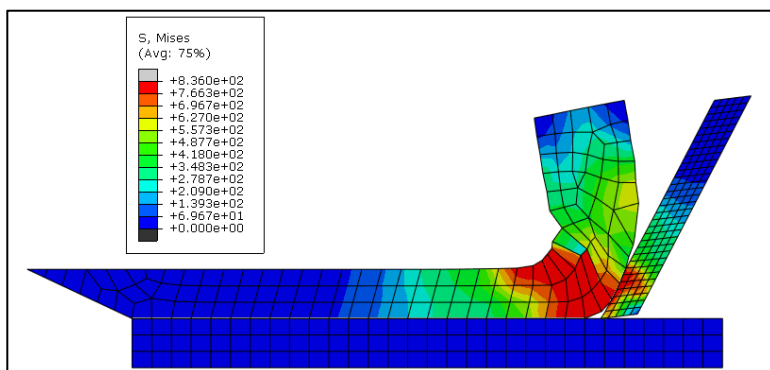


Figure 5. Initiation of chip curl (Travel = 0.62 mm.)

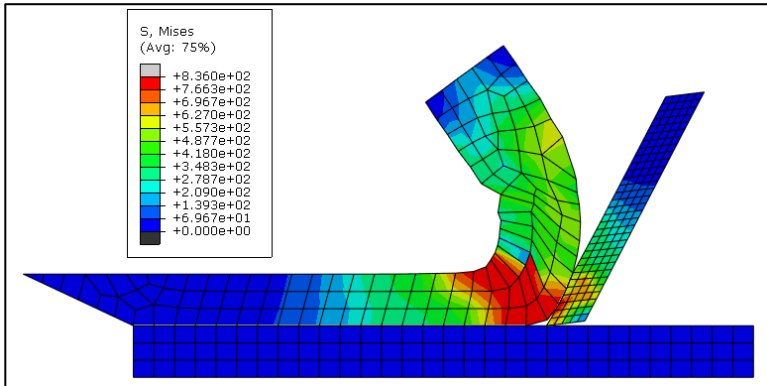


Figure 6. Cutting proceeds (Travel = 1.0 mm.)

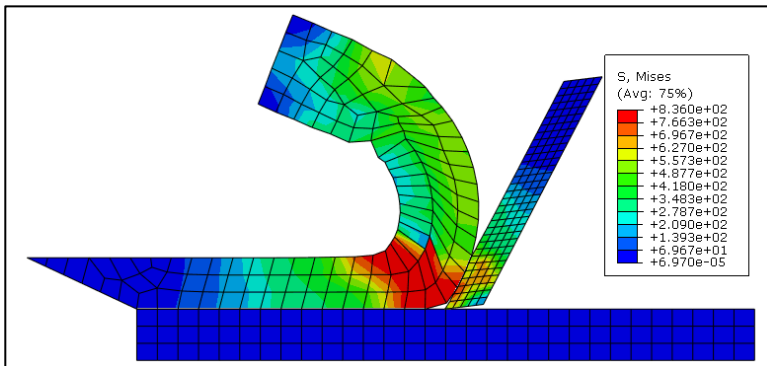


Figure 7. Cutting proceeds (Travel = 1.5 mm.)

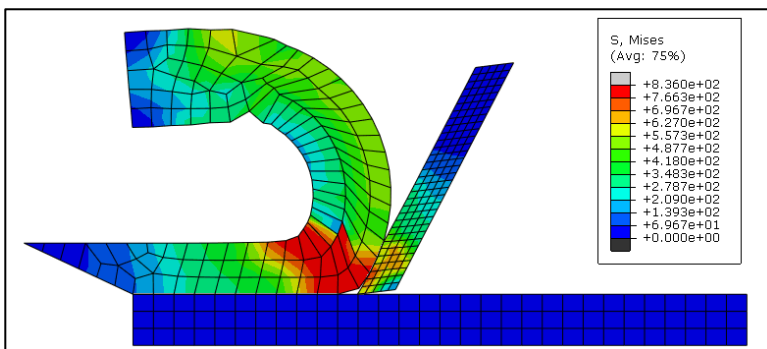


Figure 8. Cutting proceeds (Travel = 1.9 mm.)

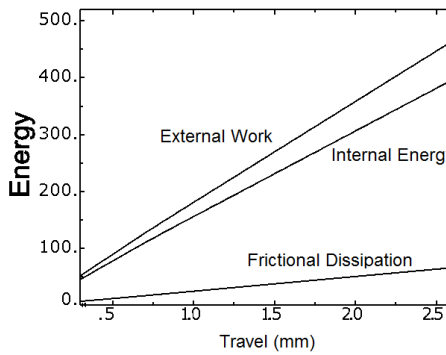


Figure 9. Energy relation

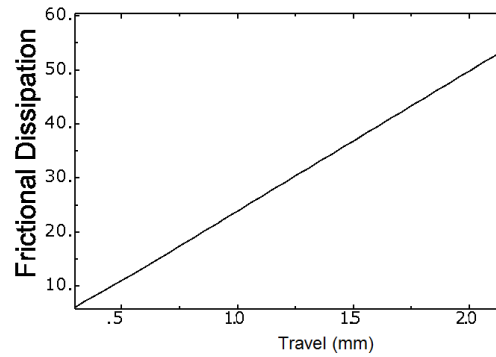


Figure 10. Frictional dissipation

6. Conclusions

A finite element analysis simulating chip formation in metal cutting was modelled. The model accounts for chip separation from the workpiece. For more accurate results in this work, the effect of spring back has been considered and the thermal effect was included in the model. The following conclusions can be drawn from the analysis:

The stress concentration at the flank face occurred as a result of the friction between the tool flank face and the machined surface added to the spring back effect was included in the model. Flank wear is well predicted as the tool wear is highly localized at the rounded part of the cutting edge (intersection between rake and flank faces) as verified by the tool wear experimental result at the same conditions. Flank wear and crater wear is actually a cumulative process increasing till tool blunt. The chip leaves the tool rake face due to chip curl as a result of the friction between chip and tool.

The FEM was verified using the experimental results of the cutting force at the same conditions of experiments. Also, the tool/workpiece interface stress on flank face is calculated and compared with the FE results where good correlation was found.

The energy relation between the external work, internal energy (plastic dissipation) and the frictional dissipation was plotted showing that the exerted external work input to the model equals to the internal energy which is the plastic dissipation added to the frictional dissipation in the rake and flank faces. The relation between the frictional dissipation and the travel of tool is very important in predicting the evolution of tool wear at any given cutting time from FEM simulations. Therefore, the presented model could be used to reduce tool wear, and



hence improve the surface roughness of the workpiece and reduce the tool change down-time through optimization of the tool geometry. The model could also be used to achieve the cutting parameters that would lead to the least tool wear.

As cutting proceeds, chip curl increases, shear angle decreases, variation of tool wear as it is commutative, fissures at the shear plane free end are continuously possibly occurs, while the stress distribution on tool face is variable with the chip curl.

References

- [1] A. Svoboda, D. Wedberg, L.E. Lindgren, "Simulation of metal cutting using a physically based plasticity model," *Model. Simul. Mater. Sci. Eng.*, vol. 18, p. 19, 2010.
- [2] J. Zhao, Z. Liu, B. Wang, J. Hu, and Y. Wan, "Tool coating effects on cutting temperature during metal cutting processes: Comprehensive review and future research directions," *Mech. Syst. Signal Process.*, vol. 150, p. 107302, 2021, doi: 10.1016/j.ymsp.2020.107302.
- [3] B. Haddag, M. Nouari, "Tool wear and heat transfer analyses in dry machining based on multi-steps numerical modelling and experimental validation," *Wear*, vol. 302, pp. 1158–1170, 2013.
- [4] A. Malakizadi, S. Cedergren, I. Sadik, and L. Nyborg, "Inverse identification of flow stress in metal cutting process using Response Surface Methodology," *Simul. Model. Pract. Theory*, vol. 60, pp. 40–53, 2016, doi: 10.1016/j.simpat.2015.09.009.
- [5] C. Montenegro, S. Abolghasem, J. C. Osorio-Pinzon, and J. P. Casas-Rodriguez, "Microstructure prediction in low and high strain deformation of Al6063 using artificial neural network and finite element simulation," *Int. J. Adv. Manuf. Technol.*, vol. 106, no. 5–6, pp. 2101–2117, 2020, doi: 10.1007/s00170-019-04704-z.
- [6] D. Zhu, X. Zhang, H. Ding, "Tool wear characteristics in machining of nickel-based super-alloys," *Int. J. Mach. Tools Manuf.*, vol. 64, pp. 60–77, 2013.
- [7] E. Sayit, K. Aslantas, A. Çiçek, "Tool Wear Mechanism in Interrupted Cutting Conditions," *Mater. Manuf. Process.*, vol. 24, no. 4, p. 2009, 2009.
- [8] M. M. El-Gallab, M. Sklad, "Machining of Al/SiC particulate metal matrix composites part III: comprehensive tool wear models, Journal of Materials Processing Technology," *J. Mater. Process. Technol.*, vol. 101, pp. 10–20,

2000.

- [9] M. Binder, F. Klocke, B. Doebbler, “An advanced numerical approach on tool wear simulation for tool and process design in metal cutting,” *Simul. Model. Pract. Theory*, vol. 70, pp. 65–82, 2017, doi: 10.1016/j.simpat.2016.09.001.
- [10] C. Mao, Z.X. Zhou, Y.H. Ren, and B. Zhang, “Analysis and FEM Simulation of Temperature Field in Wet Surface Grinding,” *Mater. Manuf. Process.*, vol. 25, no. 6, pp. 399–406, 2010, [Online]. Available: <http://dx.doi.org/10.1016/j.tplants.2011.03.004><http://dx.doi.org/10.1016/j.pbi.2010.01.004><http://www.biomedcentral.com/1471-2156/12/42><http://dx.doi.org/10.1016/j.biotechadv.2009.11.005><http://www.sciencemag.org/content/323/5911/240.short>
- [11] B. S. Wang, J. M. Zuo, M. L. Wang, and J. M. Hou, “Prediction of Milling Force Based on Numerical Simulation of Oblique Cutting,” *Mater. Manuf. Process.*, vol. 27, no. 10, pp. 1011–1016, 2012.
- [12] Q. Xia, D. R. Gillespie, “Quasi-static finite element modelling of thermal distribution and heat partitioning for the multi-component system of high speed metal cutting,” *J. Mater. Process. Technol.*, vol. 275, no. August 2019, p. 116389, 2020, doi: 10.1016/j.jmatprotec.2019.116389.
- [13] B. Li, “A review of tool wear estimation using theoretical analysis and numerical simulation technologies,” *Int. J. Refract. Met. Hard Mater.*, vol. 35, pp. 143–151, 2012.
- [14] Y. Yen, J. Söhner, B. Lilly, and T. Altana, “Estimation of tool wear in orthogonal cutting using the finite element analysis,” *J. Mater. Process. Technol.*, vol. 146, pp. 82–91, 2004.
- [15] A. Attanasio, E. Ceretti, A. Fiorentino, C. Cappellini, and C. Giardini, “Investigation and FEM-based simulation of tool wear in turning operations with uncoated carbide tools,” *Wear*, vol. 269, pp. 433–350, 2010.
- [16] D. Yang, Z. Liu, X. Ren, and P. Zhuang, “Hybrid modeling with finite element and statistical methods for residual stress prediction in peripheral milling of titanium alloy Ti-6Al-4V,” *Int. J. Mech. Sci.*, vol. 108–109, pp. 29–38, 2016, doi: 10.1016/j.ijmecsci.2016.01.027.
- [17] T. Thepsonthi, T. Özel, “Experimental and finite element simulation based investigations on micro-milling Ti-6Al-4V titanium alloy: Effects of cBN coating on tool wear,” *J. Mater. Process. Technol.*, vol. 213, pp. 532–542,



2013.

- [18] A. Vadiraj, M. Kamaraj, V. S. Sreenivasan, “Effect of sliding speed on wear behaviour of nitrided martensitic stainless steel under boric acid and MoS₂ lubrication,” *Surf. Eng.*, vol. 28, no. 3, pp. 192–194, 2012.
- [19] W. Grzesik, P. Nieslony, “Coupled thermo-mechanical FEM-based modelling of the tool-chip contact behaviour for coated cutting tools,” *Int. J. Mach. Mach. Mater.*, vol. 11, no. 1, pp. 20–35, 2012.
- [20] J. Lorentzon, N. Järvestråt, “Modelling tool wear in cemented-carbide machining alloy,” *Int. J. Mach. Tools Manuf.*, vol. 48, pp. 1072–1080, 2008.
- [21] E. Usui, T. Shirakhashi, T. Kitagawa, “Part 3: Analytical prediction of three dimensional cutting process,” *Trans. ASME, J. Eng. Ind.*, no. 1, pp. 33–38, 1978.
- [22] C. Arcona, T. A. Dow, “An Empirical Tool Force Model for Precision Machining,” *Trans. ASME, J. Manuf. Sci. Eng.*, vol. 120, pp. 700–707, 1998.
- [23] F.Z. Fang, H. Wu, Y.C. Liu, “Modelling and experimental investigation on nanometric cutting of monocrystalline silicon,” *Int. J. Mach. Tools Manuf.*, vol. 45, pp. 1681–1686, 2005.
- [24] F. Ozturk, R.E. Ece, N. Polat, and A. Koksall, “Effect of Warm Temperature on Springback Compensation of Titanium Sheet,” *Mater. Manuf. Process.*, vol. 25, no. 9, p. 2010, 2010.
- [25] C. P. Jiang, C.C. Chen, “Grain Size Effect on the Springback Behavior of the Microtube in the Press Bending Process,” *Process. Mater. Manuf.*, vol. 27, no. 5, p. 2012, 2012.
- [26] F. Ducobu, E. Rivière-Lorphèvre, E. Filippi, “Finite element modelling of 3D orthogonal cutting experimental tests with the Coupled Eulerian-Lagrangian (CEL) formulation,” *Finite Elem. Anal. Des.*, vol. 134, no. May, pp. 27–40, 2017, doi: 10.1016/j.finel.2017.05.010.
- [27] S. K. Mishra, S. Ghosh, S. Aravindan, “3D finite element investigations on textured tools with different geometrical shapes for dry machining of titanium alloys,” *Int. J. Mech. Sci.*, vol. 141, no. March, pp. 424–449, 2018, doi: 10.1016/j.ijmecsci.2018.04.011.
- [28] R.G. Fenton, P. L. B. Oxley, “Predicting Cutting Forces at Super High Cutting Speeds From Work Material Properties and Cutting Conditions,” *n Adv. Mach. Tool Des. Res.*, pp. 247–258, 1967.

- [29] N. El Chazly, M.S.M. Riad, M.A. Adly, and T. M. El-Hossainy, "Finite Element Model for High Speed Machining," *Int. Conf. Mech. Des. Prod.*, pp. 199–200, 1996.
- [30] "Handbook of High-Speed Machining Technology," *Publ. by Chapman Hall, USA*, p. 1985, 1985.
- [31] C.R. Friedrich, V. P. Kulkarni, "Effect of workpiece springback on micromilling forces. Microsystem Technologies," *Microsyst. Technol.*, vol. 10, pp. 472–477, 2004.
- [32] M. Arif, Z. Xinquan, M. Rahman, and S. Kumar, "A predictive model of the critical undeformed chip thickness for ductile–brittle transition in nanomachining of brittle materials.," *Int. J. Mach. Tools Manuf.*, vol. 64, pp. 114–122, 2013.
- [33] D. MARSHAL, "Indentation of Brittle Materials, Microindentation Techniques in Materials Science and Engineering," *Amer. Soc. Test. Mater.*, pp. 26–46, 1986.